

MULTISCALE MODELLING OF TEXTILE COMPOSITES STRUCTURES USING MECHANICS OF STRUCTURE GENOME

Xin Liu¹, Khizar Rouf¹ and Wenbin Yu¹

¹ School of Aeronautics and Astronautics, Purdue University, West Lafayette, IN, USA, 47907-2045,
Email: wenbinyu@purdue.edu and <https://cdmhub.org/groups/yugroup>

Keywords: Textile composites, Multiscale structural modelling, Mechanics of structure genome

ABSTRACT

Mechanics of structure genome (MSG) is extended to provide a new multiscale modelling approach for textile composites. MSG decouples the original complex structural analysis of textile composites into homogenization analysis, macroscopic structural analysis and dehomogenization analysis. For homogenization analysis, effective yarn properties are obtained from fiber and matrix properties in first homogenization step (micro-homogenization). In the second homogenization step (macro-homogenization), different constitutive relations of textile composites are computed from the yarn and matrix properties based on MSG solid model, plate model and beam model. The constitutive relations obtained from homogenization analysis are applied in the macroscopic structural analysis, and then the corresponding structural responses are used as inputs for dehomogenization analysis for the local fields. The predictions using MSG plate and beam model are compared with direct numerical simulation (DNS) using 3D FEA. The results show effective material properties using MSG solid model can give the same accuracy as 3D RVE analysis and greatly improve the computational efficiency. By using MSG plate and beam models, both the global behaviour and local fields can be accurately predicted compared with DNS results with much less computing cost and modelling effort.

1 INTRODUCTION

Textile composites not only inherit the advantages of unidirectional composites, such as light weight and high specific strength, but also possess higher interlaminar shear strength, better damage tolerance and impact resistance as compared to unidirectional composites. However, due to the complex microstructures, the behaviours of textile composites are difficult to be accurately predicted, capturing the details of textile microstructures. Engineers usually use homogenized properties obtained from a typical pattern of textile composites for structural modelling.

In order to predict the effective elastic properties of textile composites, many models have been proposed during the last several decades. Ishikawa and Chou [1-2] proposed different analytical models to predict the homogenized response of woven fabric composites (WFCs) in 1980s. The models were based on the classical lamination theory (CLT) combined with iso-strain or iso-stress assumptions. Later, many models were developed using the similar assumptions or mixed iso-strain/iso-stress assumptions [3]. One significant improvement for analytical model was proposed by Gommers et al. [4], which was based on the inclusion method that removes the iso-stress/strain assumptions. This method has been implemented in the commercialized software WiseTex. Although analytical models provide good estimation of the in-plane properties, they are not good at predicting the shear and out-of-plane properties of textile composites. In addition to that, due to the various assumptions made in the contemporary analytical models, it is hard to find a unified analytical model that is applicable to all possible textile microstructures. In addition to analytical models, the finite element analysis (FEA) based numerical models have been widely used to study the two-dimensional (2D) and 3D textile composites [5-6]. Compared with analytical models, numerical models usually provide better predictions for both effective properties and local fields. However, numerical models of complex 3D textiles requires significant resources and time.

As many structures in engineering are very thin or slender, engineers usually prefer to model these structures using shell or beam elements, which simplifies the model as one-dimensional (1D) or 2D models depending on the geometric characteristics of the original model. For the plate textile

composite model, classical laminate plate theory (CLPT) is widely used to predict \mathbf{A} , \mathbf{B} and \mathbf{D} matrices for plate constitutive relation. The early works were still performed by Ishikawa and Chou [2, 7], who conducted earlier analytical predictions using CLPT. In these predictions, 2D woven composites were modelled in series and parallel based on the loading direction, and \mathbf{A} , \mathbf{B} and \mathbf{D} matrices were predicted. Later, many models based on CLPT on different 2D and 3D woven textiles are proposed. However, different assumptions must be made for dealing with different types of textile composites using this kind of analytical approaches. The other set of models trying to get the effective properties of textile plate using the numerical method by applying in-plane periodic boundary conditions (PBCs), and in this way, textile composites with different geometries can be modelled using the same approach. Marrey and Sankar [8] has pointed out that the \mathbf{B} and \mathbf{D} matrices are not able to be accurately predicted using homogenized elastic properties. There are not many available beam models for textile structures, part of the reasons are due to the complexity of forming such models. Sankar and Marrey [9] proposed a finite element based model to predict beam stiffness matrix. In this analysis, they implemented PBCs on the unit cell faces and applied three independent deformations (pure extension, pure bending, and pure shear) to predict the beam stiffness coefficients.

In this paper, mechanics of structure genome (MSG) is extended to provide a unified approach for modelling textile composites using solid, plate and beam models. MSG was recently discovered as a unified approach for multiscale constitutive modelling of heterogeneous structures and materials [10]. By using the principle of minimum information loss (PMIL), MSG introduces no ad hoc assumptions and guarantees the accuracy of the results [11]. Another advantage of MSG is that it unifies micromechanics and structural mechanics, which has the possibility to predict structural properties in terms of microstructures without invalid scale separation. MSG-based structural modelling has been demonstrated to be an efficient and accurate approach to model various engineering structures with complex geometry made of composites [12-13]. MSG has been implemented in a general-purpose multiscale constitutive modeling software SwiftComp™, which takes the geometry and material characteristics of a Structure Genome (SG) [14] as the input and computes the constitutive models for the macroscopic structural analysis. After analyzing structural responses, SwiftComp™ can also perform dehomogenization to predict the local fields.

2 MSG MULTISCALE MODELING FRAMEWORK

2.1 MSG solid, plate and beam model

As mentioned in the last section, MSG can directly provide the constitutive relations needed for different structural elements (e.g. solid, plate/shell and beam). For solid model, the constitutive relation is the 6 by 6 stiffness matrix. For MSG plate model, the constitutive relation is 6 by 6 plate stiffness matrix which consists of \mathbf{A} , \mathbf{B} and \mathbf{D} matrices. For MSG beam model, the constitutive relation is 4 by 4 stiffness matrix. These corresponding constitutive relations can be written as

$$\begin{Bmatrix} \sigma_{11} \\ \sigma_{22} \\ \sigma_{33} \\ \sigma_{23} \\ \sigma_{13} \\ \sigma_{12} \end{Bmatrix} = \begin{bmatrix} C_{11} & C_{12} & C_{13} & C_{14} & C_{15} & C_{16} \\ C_{12} & C_{22} & C_{23} & C_{24} & C_{25} & C_{26} \\ C_{13} & C_{23} & C_{33} & C_{34} & C_{35} & C_{36} \\ C_{14} & C_{24} & C_{34} & C_{44} & C_{45} & C_{46} \\ C_{15} & C_{25} & C_{35} & C_{45} & C_{55} & C_{56} \\ C_{16} & C_{26} & C_{36} & C_{46} & C_{56} & C_{66} \end{bmatrix} \begin{Bmatrix} \epsilon_{11} \\ \epsilon_{22} \\ \epsilon_{33} \\ 2\epsilon_{23} \\ 2\epsilon_{13} \\ 2\epsilon_{12} \end{Bmatrix} \quad (1)$$

$$\begin{Bmatrix} N_{11} \\ N_{22} \\ N_{12} \\ M_{11} \\ M_{22} \\ M_{12} \end{Bmatrix} = \begin{bmatrix} A_{11} & A_{12} & A_{16} & B_{11} & B_{12} & B_{16} \\ A_{12} & A_{22} & A_{26} & B_{12} & B_{22} & B_{26} \\ A_{16} & A_{26} & A_{66} & B_{16} & B_{26} & B_{66} \\ B_{11} & B_{12} & B_{16} & D_{11} & D_{12} & D_{16} \\ B_{12} & B_{22} & B_{26} & D_{12} & D_{22} & D_{26} \\ B_{16} & B_{26} & B_{66} & D_{16} & D_{26} & D_{66} \end{bmatrix} \begin{Bmatrix} \epsilon_{11} \\ \epsilon_{22} \\ 2\epsilon_{12} \\ \kappa_{11} \\ \kappa_{22} \\ 2\kappa_{12} \end{Bmatrix} \quad \begin{Bmatrix} F_1 \\ M_1 \\ M_2 \\ M_3 \end{Bmatrix} = \begin{bmatrix} S_{11} & S_{12} & S_{13} & S_{14} \\ S_{12} & S_{22} & S_{23} & S_{24} \\ S_{13} & S_{23} & S_{33} & S_{34} \\ S_{14} & S_{24} & S_{34} & S_{44} \end{bmatrix} \begin{Bmatrix} \gamma_{11} \\ \kappa_1 \\ \kappa_2 \\ \kappa_3 \end{Bmatrix} \quad (2)$$

The solid and plate constitutive relations can also be written in the matrix form

$$\{\sigma\} = [C]\{\varepsilon\} \quad \begin{Bmatrix} N \\ M \end{Bmatrix} = \begin{bmatrix} A & B \\ B^T & D \end{bmatrix} \begin{Bmatrix} \epsilon \\ \kappa \end{Bmatrix} \quad (3)$$

where $\{\sigma\}$ and $\{\varepsilon\}$ are the stress and strain components, $\{N \ M\}^T$ are the plate stress resultants, $\{\epsilon \ \kappa\}^T$ are the plate in-plane strains and curvatures. $\{F_1 \ M_1 \ M_2 \ M_3\}^T$ are the beam stress resultants, $\{\gamma_{11} \ \kappa_1 \ \kappa_2 \ \kappa_3\}^T$ are the extension strain and curvatures for the beam model.

2.2 MSG multiscale modelling framework

Figure 1 shows the framework for MSG-based multiscale modelling. The properties of individual constituent (e.g. fibers and matrix) are treated as inputs for obtaining effective properties of yarns. Then, the constitutive relation of different structures (e.g. beam, plate/shell and solid) can be computed based on effective yarn properties and matrix properties, which are later used for structural analysis. If a structure has one dimension that is much larger than the other two dimensions, then the structure can be analysed by MSG beam model. If a structure has one dimension that is much smaller than the other two dimensions, then this structure is can be analysed using MSG plate model. If the three dimensions of a structure are of similar size, then this structure can be analysed by MSG solid model. After structural analysis, the local stress/strain fields can be obtained by MSG dehomogenization analysis.

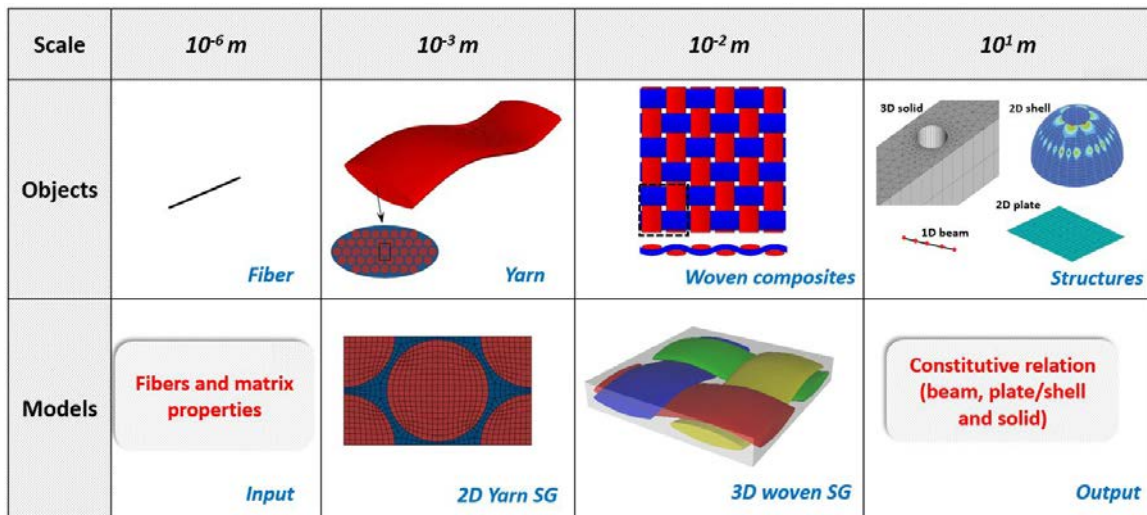


Figure 1. MSG-Based Multiscale Structural Modeling of Textile Composites

3 MSG MULTISCALE HOMOGENIZATION USING SOLID MODEL

MSG offers several advantages over the contemporary approaches in predicting the effective material properties of textile composites. Compared with analytical approaches, MSG discretizes the analysis domain using finite elements, the local material orientation is described using element local coordinates instead of using some prescribed functions in most analytical approaches. Additionally, MSG provides a unified approach to deal all kinds of textile composites, because arbitrary microstructure can be accurately described using finite element meshes. The above two issues may also be solved by the RVE analysis using 3D FEA, but MSG also has some advantages over RVE analysis. First, applying the right boundary conditions is crucial for RVE analysis and it is not always straightforward. On the contrary, one can directly use MSG to compute effective properties without applying boundary conditions manually. Second, RVE analysis usually requires the periodicity in three directions. However, for very thin textile composites the periodicity requirement is not satisfied in the thickness direction. In this case, applying the right boundary conditions to get the complete set

of 3D properties is not trivial in RVE analysis. However, MSG can easily handle aperiodic boundary condition (aPBCs) in any directions for textile composites [15]. Third, as MSG is a semi-analytical approach, the computational time is much faster than the 3D RVE analysis.

A two-step homogenization approach is used to obtain the effective properties of textile composites. To use MSG, we need to identify SG, which is similar as other micromechanics approaches to identifying RVE. As mentioned in the previous section, the yarn properties can be obtained by a 2D SG instead of a 3D RVE which can reduce the computational time without loss of accuracy. At microscale level, we compute the effective properties of the yarn which is composed by the fibers and matrix using a 2D SG. Then we use the effective yarn properties and matrix properties to compute the effective properties of the textile composite using a 3D SG. Since the textile composites are usually made by a fixed repeating pattern, the SG for macro-homogenization analysis is also easy to identify.

3.1 Micro-homogenization for yarns

Three models are presented in this section: elliptical yarn cross-section model with aPBCs, 2D square pack SG model with PBCs and 3D RVE model with PBCs as shown in Figure 2. The constituent properties (carbon fiber (T-300) and epoxy resin-3601) are kept identical across three models, which are taken from [17]. The constituent properties are presented in Table 1.

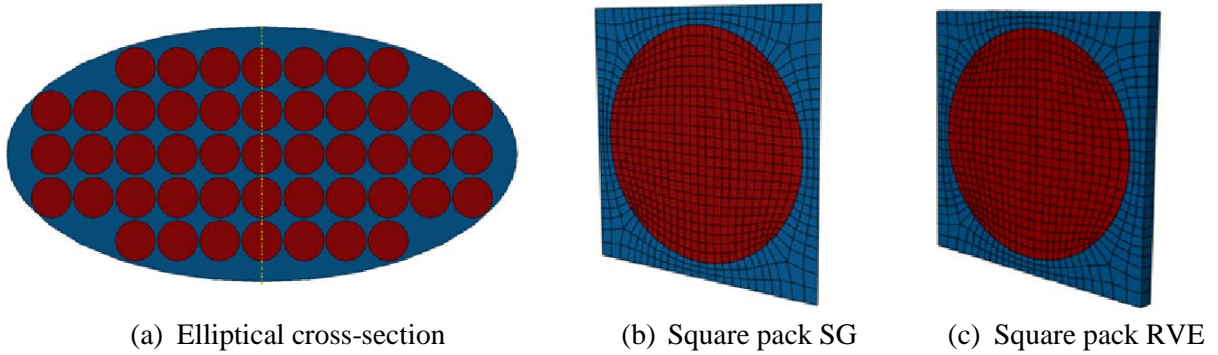


Figure 2: Yarn models.

Engineering constant		Matrix	Fiber
E_1	[GPa]	4.51	208.80
$E_2 = E_3$	[GPa]	4.51	43.00
$G_{12} = G_{13}$	[GPa]	1.70	7.42
G_{23}	[GPa]	1.70	7.42
$\nu_{12} = \nu_{13}$	–	0.38	0.20
ν_{23}	–	0.38	0.50

Table 1: Fiber and matrix properties.

For the elliptical yarn cross-section model, yarns having different numbers of fibers were modelled using 2D SGs. Nine models having different number of fibers 2, 6, 12, 24, 47, 100, 200, 300 and 400 were modelled for homogenization. Fiber diameter was changed to maintain fiber volume ratio equal to 60%. After meshing, homogenization was conducted by applying aPBCs. For the 2D square pack SG, fiber volume fraction and constituent properties were exactly the same as in the elliptical models. The dimensions of SG were 1 unit \times 1 unit. 3D RVE analysis of yarn was conducted as the reference model to compare with the other two MSG models. The dimensions of RVE were 1 unit \times 1 unit \times 0.05 unit. The fiber volume ratio and constituent properties were kept the same as in the other two approaches. The mesh size was kept the same in the planar directions as for 2D SG.

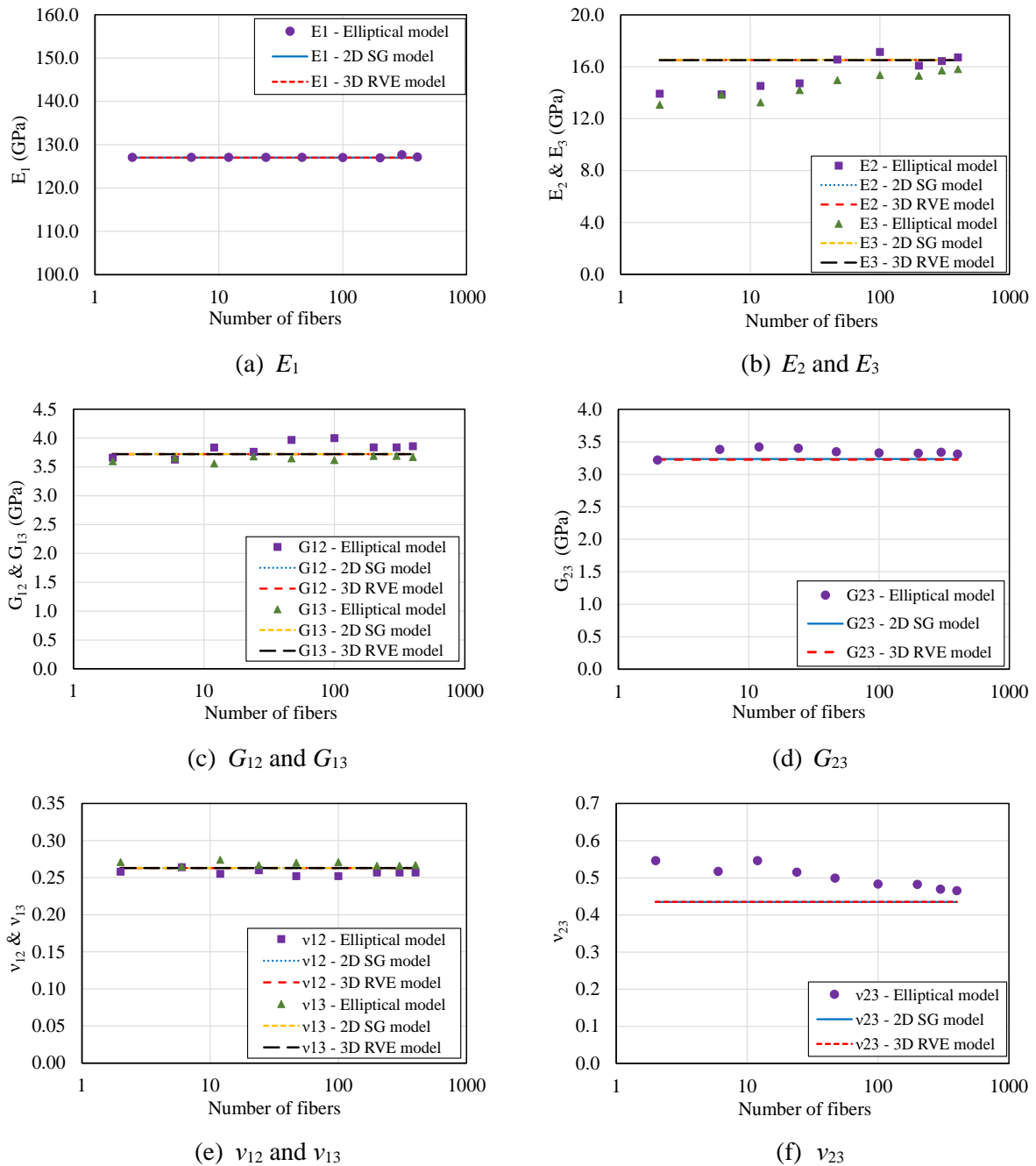


Figure 3: Predicted engineering constants using three different models

All nine elastic constants were plotted on log (number of fibers) - linear (elastic constant) scale in Figure 3. It is easy to conclude that all the engineering constants of 2D SG model and 3D RVE model agree well. For the elliptical yarn model, it can be seen from Figure 3(a) that increasing number of fibers has almost negligible impact on the longitudinal elastic modulus E_1 . It is insensitive when the number of fibers is changed. This is in support to the earlier finding that fiber distribution has least impact on the longitudinal elastic modulus [18]. As the number of fibers was increased in the elliptical model, the Young's modulus E_2 and E_3 increased towards the values based on 3D RVE and 2D SG models. All the shear moduli were found to be insensitive to the number of fibers in elliptical model. A good agreement among the shear moduli predicted by three models was seen in Figure 3(c,d). ν_{12} and ν_{13} remains almost insensitive when the number of fibers was increased in the elliptical yarn model. However, the values of ν_{23} is very sensitive to the number of fibers, and the value approaches

the results of other models as the number of fibers increasing.

Based on the results obtained by three approaches, it is clear that MSG based yarn modelling approach with aPBCs can be used to predict 3D properties of yarns having arbitrary shape and having arbitrary number of fibers. This tool can be used to analyze 3D properties of real yarns having random fiber distributions. Further, this tool can be very helpful in predicting the homogenized response of hybrid yarns (yarns having more than one type of fibers).

3.2 Macro-homogenization for textile composites

Once the properties of yarns are obtained from micro-homogenization analysis, we are ready to perform a macro-homogenization analysis to compute the properties of the textile composites. The properties of yarn and matrix are given in Table 2 which are obtained by MSG 2D SG model from last section.

Engineering constant		Matrix	Yarn
E_1	[GPa]	4.51	126.91
$E_2 = E_3$	[GPa]	4.51	16.49
$G_{12} = G_{13}$	[GPa]	1.70	3.72
G_{23}	[GPa]	1.70	3.22
$\nu_{12} = \nu_{13}$	–	0.38	0.26
ν_{23}	–	0.38	0.44

Table 2: Elastic properties of yarn and matrix.

In order to demonstrate the accuracy and efficiency of MSG, the same models with identical mesh size and element type are used for 3D RVE analysis. The difference of the results using MSG and 3D RVE with PBCs are compared with the following equation:

$$\text{Diff1} = \frac{|\text{MSG results} - \text{3D RVE results}|}{\text{3D RVE results}} \times 100\% \quad (6)$$

The first example is a plain weave textile composites structure. The typical plain weave and the corresponding SG is shown in Figure 4. The SG contains 2 warp yarns and 2 weft yarns. The yarn spacing is 1 unit and yarn width is 0.8 unit. The fabric thickness is 0.2 unit and the yarn has an elliptical cross section. The 3D model contains 16,000 8-noded brick elements generated using TexGen4SC. Table 3 presents the results using MSG and 3D RVE models.

In addition to 2D woven composites, 3D woven composites are widely used in recent years due to the improved properties in the transverse direction and high production speed which reduces the manufacturing cost and cycle times. A 3D model of orthogonal woven composites is built as shown in Figure 5. The model contains 3 layers with 2 weft yarns in each layer. The weft yarn spacing is 1 unit, yarn width is 0.8 unit and yarn height is 0.1 unit. There are 2 layers with 2 warp yarns in each layer and 1 binder yarn. The warp yarn spacing is 1 unit, yarn width is 0.8 unit and yarn height is 0.1 unit. The cross sections of all the yarns in this model are elliptical cross sections. The model contains 50,000 8-noded brick elements and the corresponding results are given in Table 4.

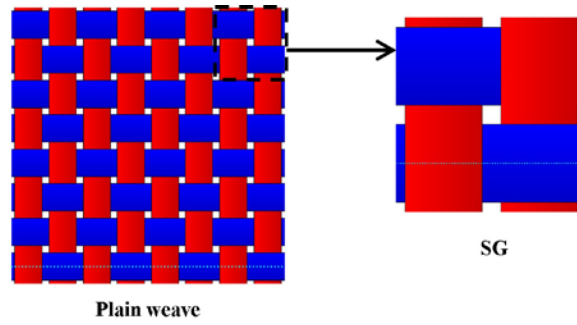


Figure 4: plain weave textile composites and its SG.

		MSG	3D FEA	Diff1 (%)
Computing time	[s]	10.782	160	
$E_1 = E_2$	[GPa]	50.261	49.952	0.619
E_3	[GPa]	14.983	14.905	0.523
G_{12}	[GPa]	3.416	3.414	0.059
$G_{13} = G_{23}$	[GPa]	3.140	3.133	0.223
ν_{12}	–	0.138	0.137	0.730
$\nu_{13} = \nu_{23}$	–	0.424	0.424	0.000

Table 3: MSG and 3D FEA results for plain weave composites

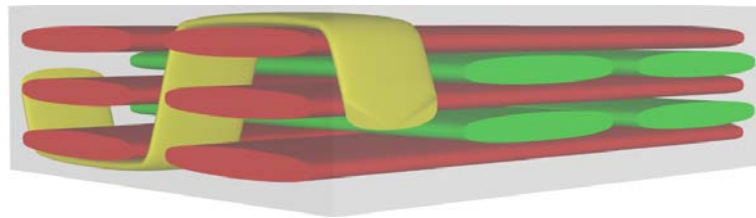


Figure 5: 3D orthogonal textile composites and its SG.

		MSG	3D FEA	Diff1 (%)
Computational time	[s]	172.85	783	
E_1	[GPa]	33.010	32.974	0.109
E_2	[GPa]	51.229	51.211	0.035
E_3	[GPa]	11.170	11.126	0.395
G_{12}	[GPa]	2.881	2.880	0.035
G_{13}	[GPa]	2.443	2.433	0.411
G_{23}	[GPa]	2.451	2.449	0.082
ν_{12}	–	0.062	0.062	0.000
ν_{13}	–	0.496	0.497	0.201
ν_{23}	–	0.454	0.456	0.439

Table 4: MSG and 3D FEA results for 3D orthogonal woven composites

All the meshes of the woven composite examples studied above are generated by TexGen4SC, and the voxel mesh is used to avoid distorted elements. However, the number of elements of a voxel mesh is required to be high to achieve accurate representation of the textile geometry [19]. This limitation results in considerable computation resources and time in 3D RVE analysis. We can conclude from the above examples that MSG computing time is much faster than 3D RVE analysis with the same mesh size. The percentage difference between MSG (PBCs) and 3D FEA is less than one percent in all properties in all the examples. In other words, MSG can provide the results as accurate as 3D RVE analysis for materials featuring 3D periodicity with greatly improved computational efficiency.

4 MSG MULTISCALE HOMOGENIZATION USING BEAM AND PLATE MODEL

The previous examples shows that the MSG solid model can predict the effective material properties with the same accuracy as 3D RVE analysis for materials featuring 3D periodicity. As mentioned in the first section, the macro-homogenization analysis is also able to calculate the beam and plate stiffness matrix which can be directly used in plate and beam elements by FEA. In this section, the stiffness matrix for beam and plate textile composites are firstly obtained from the macro-homogenization analysis, then the corresponding structural analysis are performed analytically or using Abaqus 6.13 with the effective beam and plate constitutive relations. After macroscale beam and plate analysis, the global responses like strains and curvatures are used as inputs to perform MSG dehomogenization, which will recover the local displacements, stress and strain fields. To demonstrate the accuracy and efficiency of MSG beam and plate model, DNS models are performed with modeling all the microstructural details of yarn geometry and varying material orientations along the yarn path.

4.1 Plain weave textile beam

In this example, a plain weave textile beam is analysed based on MSG beam model. It was constrained as a cantilever, and the uniform pressure of magnitude 0.01 MPa in the negative x_3 direction was applied. This structure consists of two plies of plain weave composite. The length, width and thickness of this structure are 3 mm, 0.3 mm and 0.04 mm respectively. To conduct MSG based analysis, the first step is to identify SG. The 3D SG is used for this beam because plain weave composite has 3D heterogeneity (see Figure 6). The dimensions of the SG are 0.3 mm \times 0.3 mm \times 0.04 mm. The SG was discretized using 86,400 20-noded brick elements. The nonzero terms of the beam stiffness matrix for this SG was computed using TexGen4SC as: $S_{11} = 4.49 \times 10^2 \text{ N}$, $S_{22} = 1.58 \times 10^{-2} \text{ N} \cdot \text{mm}^2$, $S_{33} = 5.64 \times 10^{-2} \text{ N} \cdot \text{mm}^2$, $S_{44} = 2.96 \text{ N} \cdot \text{mm}^2$, $S_{14} = S_{41} = 2.52 \times 10^{-2} \text{ N} \cdot \text{mm}$.

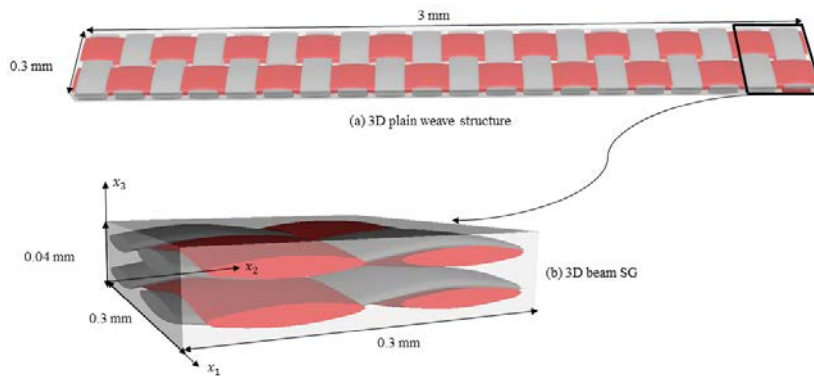


Figure 6: Plain weave composite beam and its SG.

The predicted beam stiffness was used as an input for the macroscopic structural analysis which can be solved analytically for this case. The obtained global structural responses such as displacements, strains and curvatures can be used further in MSG dehomogenization to recover the local displacements, strains and stresses of the original structure. To compare the efficiency and accuracy of MSG based beam analysis, 3D FEA of the original plain weave beam-like structure was conducted using Abaqus 6.13. This 3D structure was discretized using 864,000 20-noded brick elements. Figure 7 shows the displacements in x_3 direction along the beam using MSG and DNS. To further evaluate the local stress field predicted by the MSG beam model, the stresses distribution along the thickness at $x_1 = 1.575 \text{ mm}$ and $x_2 = 0.075 \text{ mm}$ plotted in Figures 8-10. Shear stress components are not presented here since they are very small compared with the normal stress components. We can conclude from the figures that both global displacements and local stresses can be accurately predicted by using the MSG beam model with similar accuracy as DNS. In terms of the computational efficiency, MSG based analysis took approximately 2 hours and 4 minutes using 1 CPU. However, 3D FEA took 7 hours and 44 minutes with 28 CPUs. It is clear that MSG can accurately and efficiently analyze plain weave beam-like textile structures.

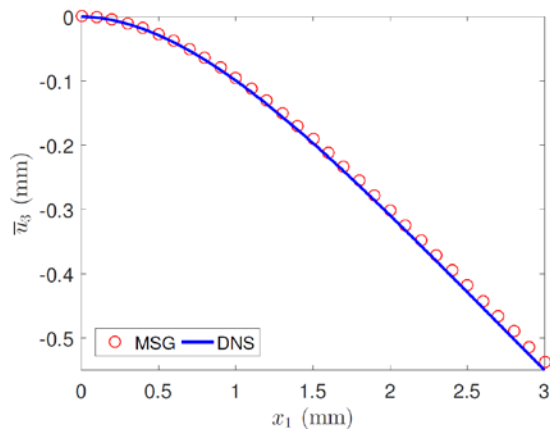


Figure 7: Deflection in plain weave beam along x_1 direction.

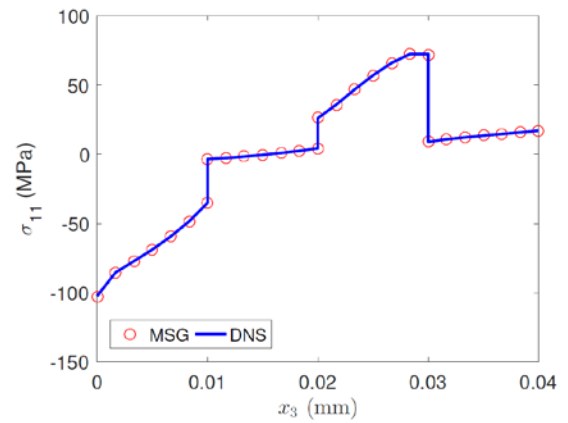


Figure 8: Distribution of σ_{11} through the thickness.

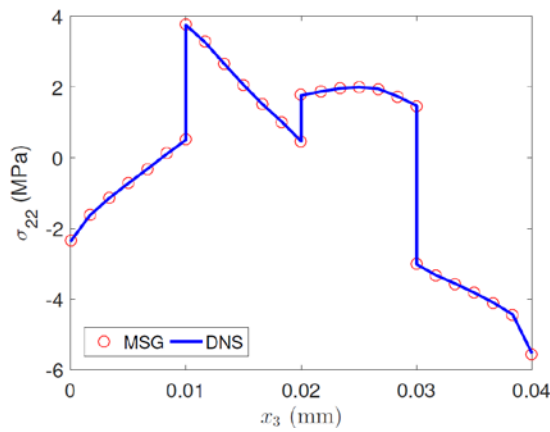


Figure 9: Distribution of σ_{22} through the thickness.

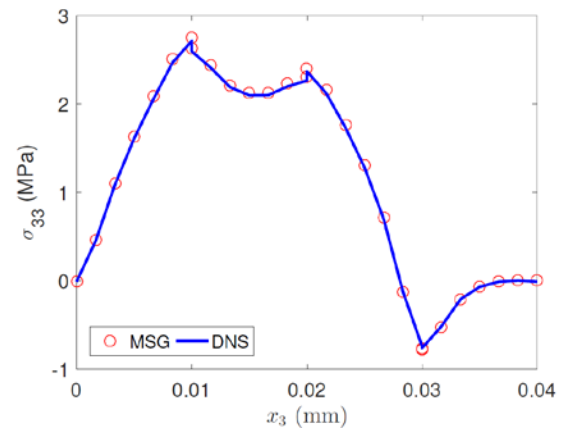


Figure 10: Distribution of σ_{33} through the thickness.

4.2 3D orthogonal textile plate

In this example, a 3D orthogonal textile plate is analysed by using the MSG plate model. This structure consists only one layer of an orthogonal textile composite. The length, width, and thickness of original structure were 3 mm, 3.6 mm and 0.07 mm respectively. The textile plate was constrained as a cantilever, and the uniform pressure of magnitude 0.01 MPa in the negative x_3 direction was applied. The first step to conduct MSG modelling is to identify the SG from the original structure. 3D SG is used in this example because this 3D orthogonal woven composite has 3D heterogeneity. The 3D SG and the original structure are shown in Figure 11. The dimensions of the SG are 0.3 mm \square 0.45 mm \square 0.07 mm. SG was discretized using 72,000 20-noded brick elements. The plate stiffness matrix was computed using TexGen4SC and the nonzero terms are: $A_{11} = 1.6 \times 10^3$ N/mm , $A_{22} = 2.8 \times 10^3$ N/mm , $A_{66} = 1.7 \times 10^2$ N/mm , $A_{12} = A_{21} = 2.0 \times 10^2$ N/mm , $D_{11} = 3.5 \times 10^{-1}$ N \cdot mm , $D_{22} = 8.1 \times 10^{-1}$ N \cdot mm , $D_{66} = 6.1 \times 10^{-2}$ N \cdot mm , $D_{12} = D_{21} = 7.0 \times 10^{-2}$ N \cdot mm .

The predicted plate stiffness matrix was used as an input for the macroscopic plate analysis to obtain the global structural responses using 3D shell element in Abaqus 6.13. The global structural responses such as strains and curvatures was used as input for MSG dehomogenization to recover the local stresses of the original heterogeneous textile plate structure. To compare the efficiency and accuracy of MSG based plate analysis, 3D FEA of the original textile plate structure was conducted using Abaqus 6.13. This 3D structure was discretized using 5.76M 20-noded brick elements. Figure 12 shows the displacements in x_3 direction along the x_1 direction of the plate using MSG model and DNS

model. To further evaluate the local stress field recovered by MSG plate model, the stresses distribution along the thickness at $x_1 = 1.575$ mm and $x_2 = 1.875$ mm is extracted and plotted in Figures 13-15. Shear stress components are not presented here since they are very small compared with the normal stress components. Based on these results, we can conclude both global displacements and local stress fields can be accurately predicted by using the MSG plate model. The results have almost the same accuracy as DNS results using 3D FEA. In terms of the computational efficiency, MSG based analysis took approximately 2 hours and 3 minutes with 1 CPU. However, 3D FEA took 20 hours and 2 minutes with 28 CPUs.

Real textile structures contain complex microstructures which usually cannot be modelled using DNS as we have just done. This is because DNS of textile composites structures require tremendous modeling efforts and computing time. The MSG-based beam and plate analysis provides a new approach to handle such structure in a much efficient way without losing accuracy.

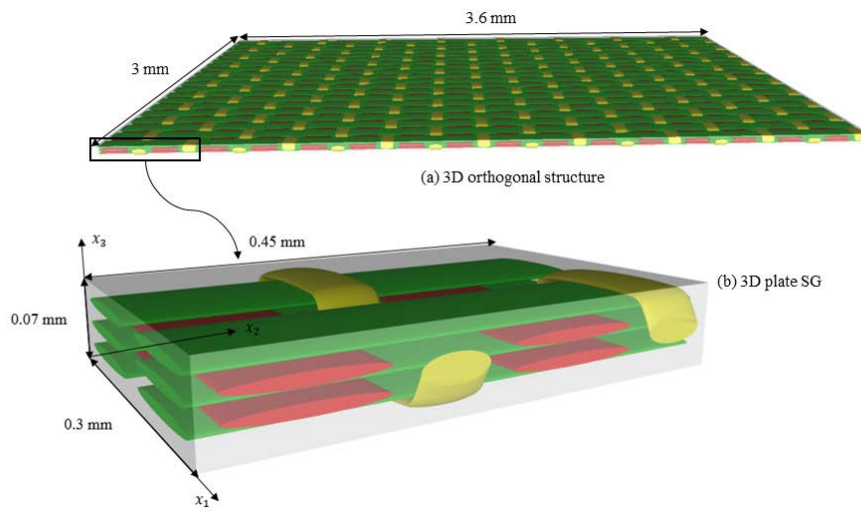


Figure 11: 3D orthogonal textile plate and its SG.

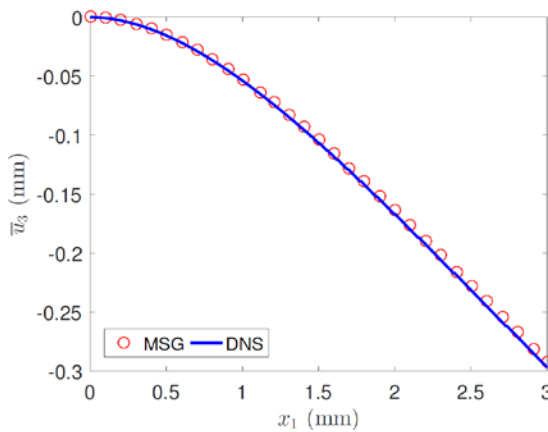


Figure 12: Deflection in 3D orthogonal textile plate along x_1 direction.

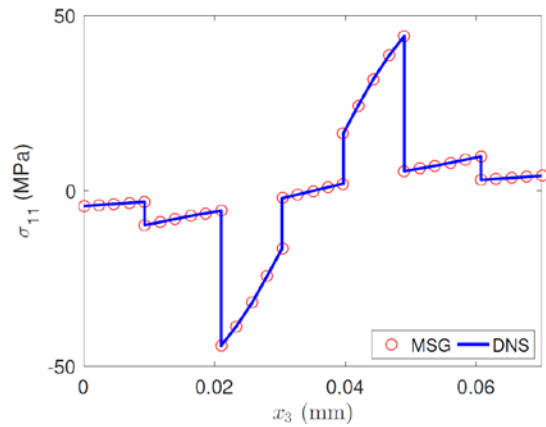


Figure 13: Distribution of σ_{11} through the thickness.

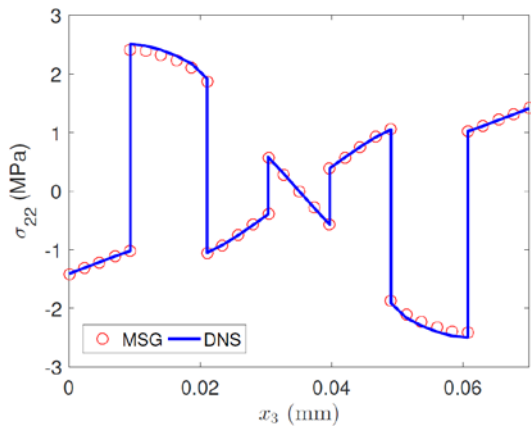


Figure 14: Distribution of σ_{22} through the thickness.

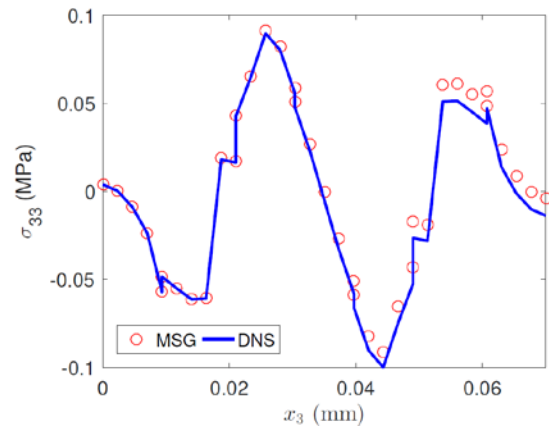


Figure 15: Distribution of σ_{33} through the thickness.

5 CONCLUSION

In this paper, a novel multiscale modeling approach is proposed to study the textile composites structures. A two-step homogenization method is used to determine the effective constitutive relation of textile composites. At the micro-scale level, homogenized yarn properties are computed considering fibers and matrix properties. MSG PBCs and aPBCs are used for studying the yarn with idealized periodic packed fibers and with the distributed fibers in an elliptical real cross section. The results show the MSG aPBC model can be used to predict 3D properties of yarns having arbitrary shape after the number of fibers increases to a certain value. At the macro-scale level, the effective yarn properties and matrix properties are first used to compute the overall effective properties of textile composites. Typical textile composite examples are analyzed to show that MSG can greatly improve the computational efficiency while maintain accuracy as 3D RVE analysis for materials featuring 3D periodicity. The macro-homogenization analysis can also generate plate and beam stiffness matrix, which can be directly used in a commercial FEA software. Examples of textile beam and plate structures are solved by MSG beam and plate model. The results of both global displacements and local stress field show excellent agreement with the results of DNS, but the computing time and modelling efforts are significantly reduced. The proposed method uses finite element to discretize the analysis domain, which means MSG provides a unified approach that is not restricted to woven fabric composites shown in this paper, but can be applied to any textile composites with arbitrary geometry. The examples in this paper are performed by a newly developed software TexGen4SC, which can be freely executed in the cloud at <https://cdmhub.org/tools/texgen4sc>. TexGen4SC is simple, general-purpose tool for efficient yet accurate design and analysis of textile composites.

ACKNOWLEDGEMENTS

The authors gratefully acknowledge the TexGen developers for providing the open source codes. We would also like to thank the Composites Design and Manufacturing HUB (cdmHUB.org) to provide the cloud platform so that users can easily access the tools generated in this work.

REFERENCES

- [1] T. Ishikawa and T.W. Chou. Elastic behaviour of woven hybrid composites, *Journal of Composites Materials*. **16**, 1982, pp. 2-19 (doi: <https://doi.org/10.1177/002199838201600101>).
- [2] T. Ishikawa and T.W. Chou. Stiffness and strength behaviour of woven fabric composites. *Journal of Materials Science*. **17**, 1982, pp. 3211-20 (doi: [10.1007/BF01203485](https://doi.org/10.1007/BF01203485)).
- [3] S.L. Angioni, M. Meo and A. Foreman, A critical review of homogenization methods for 2D woven composites, *Journal of Reinforced Plastics and Composites*. **42**, 2011, pp. 1895-906 (doi: <https://doi.org/10.1177/0731684411408158>).

- [4] B. Gommers, I. Verpoest and P. Van Houtte, The Mori–Tanaka method applied to textile composite materials, *Acta Materialia*. **46**, 1998, pp. 2223-35 (doi: [http://doi.org/10.1016/S1359-6454\(97\)00296-6](http://doi.org/10.1016/S1359-6454(97)00296-6)).
- [5] J. Whitcomb and K. Woo, Enhanced direct stiffness method for finite element analysis of textile composites. *Composite structures*. **28(4)**, 1994, pp. 385-390 (doi: [https://doi.org/10.1016/0263-8223\(94\)90120-1](https://doi.org/10.1016/0263-8223(94)90120-1)).
- [6] S.V. Lomov, D.S. Ivanov, I. Verpoest, M. Zako, T. Kurashiki, H. Nakai, J. Molimard and A. Vautrin, Full-field strain measurements for validation of meso-FE analysis of textile composites, *Composites Part A: Applied science and manufacturing*. **39(8)**, 2008, pp. 1218-1231 (doi: <http://doi.org/10.1016/j.compositesa.2007.09.011>).
- [7] T.W. Chou and T. Ishikawa, One-dimensional micromechanical analysis of woven fabric composites, *AIAA journal*. **21(12)**, 1983, pp. 1714-1721 (doi: <http://dx.doi.org/10.2514/3.8314>).
- [8] B. R. V. Marrey and B. V. Sankar, A micromechanical model for textile composite plates, *Journal of Composite Materials*. **31(12)**, 1997, pp. 1187-1213 (doi: <https://doi.org/10.1177/002199839703101202>).
- [9] B. V. Sankar and R. V. Marrey, A unit-cell model of textile composite beams for predicting stiffness properties, *Composites Science and Technology*. **49(1)**, 1993, pp. 61-69 (doi: [https://doi.org/10.1016/0266-3538\(93\)90022-9](https://doi.org/10.1016/0266-3538(93)90022-9)).
- [10] W. Yu, A unified theory for constitutive modeling of composites, *Journal of Mechanics of Materials and Structures*. **11(4)**, 2016, pp. 379-411 (doi: [10.2140/jomms.2016.11.379](http://dx.doi.org/10.2140/jomms.2016.11.379)).
- [11] W. Yu, *An introduction to micromechanics*, in: Applied Mechanics of Materials, Vol. 828, 2016, pp. 3-4.
- [12] X. Liu and W. Yu, A novel approach to analyze beam-like composite structures using mechanics of structure genome, *Advances in Engineering Software*. **100**, 2016, pp. 238-251 (doi: <http://doi.org/10.1016/j.advengsoft.2016.08.003>).
- [13] B. Peng, J. Goodsell, R. B. Pipes and W. Yu, Generalized free-edge stress analysis using mechanics of structure genome, *Journal of Applied Mechanics*. **83**, 2016, pp. 101013 (doi: [10.1115/1.4034389](http://dx.doi.org/10.1115/1.4034389)).
- [14] W. Yu, Structure genome: fill the gap between materials genome and structural analysis, *Proceedings of 56th AIAA/ASCE/AHS/ASC Structures, Structural Dynamics, and Materials Conference*, Kissimmee, Florida, January 5-9, 2015.
- [15] X. Liu, K. Rouf, B. Peng, and W. Yu, Two-step homogenization of textile composites using mechanics of structure genome. *Composite Structures*, **171**, 2017, pp. 252-262 (doi: <http://doi.org/10.1016/j.compstruct.2017.03.029>).
- [16] H. Lin, L.P. Brown, and A.C. Long. *Modelling and simulating textile structures using TexGen*. Advanced Materials Research, Vol. 331. Trans Tech Publications, 2011.
- [17] K. Kirane, M. Salviato and Z.P. Bazant, Microplane triad model for simple and accurate prediction of orthotropic elastic constants of woven fabric composites, *Journal of Composite Materials*. **50(9)**, 2016, pp. 1247-1260 (doi: <https://doi.org/10.1177/0021998315590264>).
- [18] J. Zeman and M. Sejnoha, Numerical evaluation of effective elastic properties of graphite fiber tow impregnated by polymer matrix, *Journal of the Mechanics and Physics of Solids*. **49(1)**, 2001, pp. 69-90 (doi: [http://doi.org/10.1016/S0022-5096\(00\)00027-2](http://doi.org/10.1016/S0022-5096(00)00027-2)).
- [19] M. Matveev, A. Long and I. Jones, Modelling of textile composites with fiber strength variability, *Composites Science and Technology*. **105**, 2014, pp. 44-50 (doi: <http://doi.org/10.1016/j.compscitech.2014.09.012>).